

## Strangeness-Changing Leptonic Decay Rates for the $\Sigma^\pm$ Hyperons\*

J. Cole, J. Lee-Franzini, and R. J. Loveless

*State University of New York at Stony Brook, Stony Brook, New York 11790*

and

C. Baltay, P. Franzini, R. Newman, H. Norton,† and N. Yeh‡

*Columbia University, New York, New York 10027*

(Received 2 April 1971)

The strangeness-changing leptonic branching ratios of the  $\Sigma^\pm$  hyperon were determined from a stopping  $K^-$  exposure in the BNL-Columbia 30-in. hydrogen bubble chamber. The ratio  $(\Sigma^- \rightarrow nev)/(\text{all } \Sigma^- \text{ decays})$  is  $(0.97 \pm 0.15) \times 10^{-3}$ , and the ratio  $(\Sigma^- \rightarrow n\mu\nu)/(\text{all } \Sigma^- \text{ decays})$  is  $(0.38 \pm 0.11) \times 10^{-3}$ . No evidence is found for  $\Delta S = \Delta Q$  violations, and an upper limit for the ratio of decay rates  $[(\Sigma^+ \rightarrow nev)/(\Sigma^- \rightarrow nev)]$  is determined to be  $< 12.6\%$  with 95% confidence.

### I. INTRODUCTION

The leptonic decay rates of the hyperons, which at first seemed surprisingly small<sup>1</sup> compared to nuclear  $\beta$  decay, are now reasonably well explained by the introduction of one phenomenological parameter, the so-called Cabibbo angle, and the assumption that hadronic current transforms like an octet.<sup>2</sup> It is, however, desirable to measure these branching ratios more accurately in order to test the theory more critically and to determine the Cabibbo parameters more precisely.

Because of various experimental difficulties in utilizing other techniques, the present knowledge of  $\Sigma^\pm$  decays comes from their observation in liquid-hydrogen bubble chambers. These rare decays have to be found among the dominant two-body  $\Sigma$  decays, which are more numerous by 3 orders of magnitude.

In this article we report our final results on the branching ratios of the strangeness-changing leptonic decays of the  $\Sigma^\pm$ . The measurement of these branching ratios is one part of a study of all of the leptonic  $\Sigma$  decays. In this study the  $\Sigma$  hyperons were produced by stopping  $K^-$  mesons in the BNL-Columbia 30-in. bubble chamber filled with liquid hydrogen. A total of 550 000 photographs was used. Two techniques were used to find leptonic decays: (a) The entire exposure was scanned twice for  $\Sigma$  decays which were identifiable as leptonic decays on the scanning table by means of their characteristic appearance, and (b) all  $\Sigma^-$  decays were measured, and the momentum of the charged decay product was used to identify leptonic decays. The measurement method yielded about 5 times as many leptonic decays as the scan. Events found by either method were used in the determination of the  $g_A/g_V$  ratio, which is reported elsewhere.<sup>3</sup>

For the measurement of the branching ratios, only the decays found by scanning were used. This is because the detection efficiency as a function of leptonic momentum is much more reliably known for the sample from the scan than for the sample obtained from the measurements. Preliminary values for the branching ratios have been given.<sup>4</sup>

### II. EXPERIMENTAL METHOD

The most copious way to produce  $\Sigma$  hyperons is by stopping  $K^-$  mesons in hydrogen. The negative  $K^-$  are absorbed at rest, yielding a  $\Sigma^-$  44.7% of the time and a  $\Sigma^+$  22.8% of the time by the reaction  $K^- + p \rightarrow \Sigma^\pm + \pi^\mp$ .<sup>5</sup> The outgoing  $\Sigma$  and  $\pi$  tracks are collinear if the  $K^-$  interacts at rest.

The major difficulty in distinguishing leptonic  $\Sigma$  decays from pionic  $\Sigma$  decays arises from the particular spectra of two- and three-body pionic decays as shown in Fig. 1. The two-body pionic decay ( $\Sigma^\pm \rightarrow n\pi^\pm$ ) gives pions with a unique momentum, 193 MeV/c, in the  $\Sigma$  center-of-mass frame; the Lorentz transformation to the lab frame results in a pion momentum that varies from 160 to 220 MeV/c. In addition, the three-body radiative pion decays ( $\Sigma \rightarrow n\pi\gamma$ ) are still significant for a pion lab momentum as low as 40 MeV/c. One distinguishing characteristic of the pion tracks is that, for momentum below 130 MeV/c, a pion cannot turn through an angle of  $180^\circ$  in the chamber because the energy loss is such that a pion will stop before turning  $180^\circ$ . In addition, at this low momentum, pions are recognizable from the specific bubble density along the track.

In an exposure of the 30-in. BNL-Columbia liquid-hydrogen bubble chamber, we stopped approximately  $5 \times 10^6$   $K^-$ , corresponding to the production of  $2 \times 10^6$   $\Sigma^-$  and  $0.9 \times 10^6$   $\Sigma^+$ . The scanners were

instructed to search for a heavily ionizing short  $\Sigma$  track at the end of a stopping  $K^-$ , collinear with the production pion. The  $\Sigma$  decay track was required to describe an arc of at least  $90^\circ$  in the chamber and appear lightly ionizing to be considered a candidate for electronic decay. For a muonic decay the  $\Sigma$  decay track was required to be "dark," to be free of any kink, and to decay into an obvious electron of less than 52-MeV/c momentum. The entire exposure was scanned twice, and a small part three times. All events found on the scan were measured and reconstructed in order to eliminate as much background as possible.

### III. NORMALIZATION

We determine the total number of  $\Sigma^-$  hyperons in the exposure by double scanning and measuring all  $\Sigma^-$  decays every 250th frame. Virtually all of these events were two-body ( $\Sigma^- \rightarrow n\pi^-$ ) decays. Corrections are made for short  $\Sigma$ 's because of the low scanning efficiency. The 13.7% of the  $\Sigma$ 's which stop in the chamber and interact at rest with protons must also be corrected for since the measurements include only visible  $\Sigma$  decays.

In addition to good visibility criteria (fiducial volume, dips, etc.) the  $\Sigma$ 's were required to have a length between 0.3 and 0.9 cm. The double-scan efficiency for these events is essentially 100%. 2389  $\Sigma^-$  events remain after all restrictions.

We ascertained the effect of the restrictions by producing 15 000 Monte Carlo events that simulate the decay chain. The  $\Sigma$  decay time was related to the length in the chamber by numerical integration of

$$t_{c.m.} = \frac{M}{C} \int_0^l \frac{dx_{lab}}{p(x)}$$

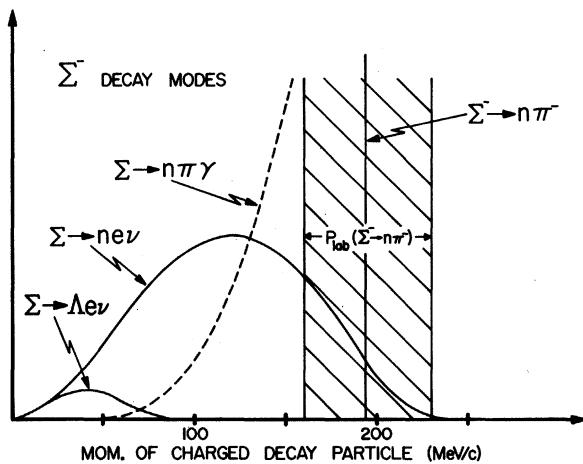


FIG. 1. Momenta spectra of two- and three-body decay modes of the  $\Sigma^-$  hyperon in the  $\Sigma^-$  center-of-mass frame.

knowing that the initial momentum of the  $\Sigma$  is 173.12 MeV/c. The Monte Carlo calculation indicates that 32.7% of the events remain after these restrictions. Hence we have  $1.82 \times 10^6$   $\Sigma^-$  produced within the fiducial volume. Using the ratio of  $\Sigma^+/\Sigma^-$ , we have  $0.85 \times 10^6$   $\Sigma^+$  produced within the fiducial volume. From a sample of 150 000  $\Sigma$  events measured in connection with the measurement of the  $g_V/g_A$  ratio, we determine the fraction of events not in the fiducial volume. We thus get a total of  $2.13 \times 10^6$   $\Sigma^-$  and  $0.99 \times 10^6$   $\Sigma^+$  in the exposure.

### IV. THE DECAY $\Sigma^- \rightarrow nev$

A total of 231 candidates for the decay  $\Sigma^- \rightarrow nev$  which were found on the scan were measured on precision measuring machines and all decay tracks were required to turn through an angle of  $180^\circ$  in the chamber, a restriction that eliminates virtually all pionic or muonic decays. Additional good-visibility constraints were made: The  $\Sigma$  vertex was required to be within the fiducial volume; the  $\Sigma$  length between 0.2 and 0.8 cm, and the  $\Sigma$  and decay-track dip angles must be less than  $60^\circ$ . A Monte Carlo calculation indicates that the effect of these additional good-visibility constraints is that 43.1% of true leptonic decays remain after such constraints, a number which is independent of the electron momentum. The double-scan efficiency of events surviving the constraints is 90%.

The distribution functions for the neutron, electron, and neutrino were computed by assuming a decay amplitude of the type

$$M = \bar{U}_n [\gamma_\mu (g_V + g_A \gamma_5) + g_W \sigma^{\mu\nu} q_\nu] \bar{U}_\Sigma \bar{U}_e \gamma_\nu (1 - \gamma_5) U_\Sigma.$$

To determine the effect of the turning-angle re-

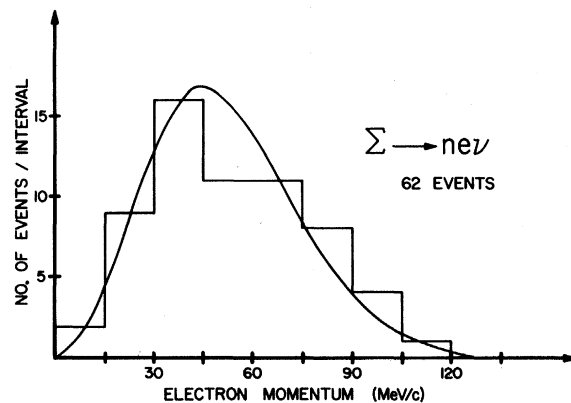


FIG. 2. Electron momentum spectrum for  $\Sigma^- \rightarrow nev$  decays where the electron turned through at least  $180^\circ$  in the chamber. The smooth curve represents the expected spectrum from a Monte Carlo calculation.

striction, the Monte Carlo program traced the electron path through the chamber in 1-cm segments until the electron track intersected the walls of the chamber. The turning angle efficiency is the percentage of electrons that turn through at least  $180^\circ$  in the 30-in. bubble chamber as a function of the momentum of the electron. The product of the theoretical electron spectrum and the turning-

angle efficiency gives the visible expected electron spectrum from  $\Sigma^-$  electronic decays. From the expected electron spectrum, one computes the fraction of all  $\Sigma$  electronic decays left after a turning angle requirement of  $180^\circ$ . Note that this visible fraction is dependent on the coupling constants because of the theoretical electron spectrum.

Background events which are not removed by the  $180^\circ$  turning-angle restriction are the decays  $\Sigma \rightarrow \Lambda e \nu$ , where the  $\Lambda$  decays via a neutral ( $\Lambda \rightarrow n \pi^0$ ) mode. The expected number of  $\Sigma \rightarrow \Lambda e \nu$  decays with no visible decay products is

$$N = R(\Sigma^- \rightarrow \Lambda e \nu) \times (\text{No. of } \Sigma^- \text{ on film}) \times (\% \text{ expected after cuts}) \times \left( \frac{\Lambda \rightarrow n \pi^0}{\text{all } \Lambda} \right) \times (\text{scan eff.}) \\ \times (\text{fraction where } e^- \text{ turns more than } 180^\circ) \\ = 5 \text{ events.}$$

Of the measured leptonic candidates, 62 survived the geometric constraints and had an electron which turned through more than  $180^\circ$  in the chamber (see Fig. 2). Since we can expect five of these events to have come from  $\Sigma \rightarrow \Lambda$  decays, 57 examples of  $\Sigma \rightarrow ne \nu$  remain. The branching ratio then is

$$R(\Sigma^- \rightarrow ne \nu) = 57 \times \frac{1}{0.431} \times \frac{1}{0.90} \times \frac{1}{1.82 \times 10^6} \times \frac{1}{\text{expected fraction}} \\ = 0.0807 \times 10^{-3} \times \frac{1}{\text{fraction where } e^- \text{ turns more than } 180^\circ}.$$

Figure 3 illustrates the dependence of the branching ratio on the  $g_A/g_V$  ratio, for various values  $g_W$ . If we choose the currently accepted values,<sup>8</sup>  $g_A/g_V = -0.30$  and  $g_W = 0.27$ , then the branching ratio becomes

$$R(\Sigma^- \rightarrow ne \nu) = (0.97 \pm 0.15) \times 10^{-3}.$$

#### V. TEST OF THE $\Delta S = \Delta Q$ RULE

According to the  $\Delta S = \Delta Q$  rule, the decay  $\Sigma^+ \rightarrow ne^+ \nu$  is prohibited while the decay  $\Sigma^- \rightarrow ne \nu$  is allowed. The search for the decays  $\Sigma^+ \rightarrow ne^+ \nu$  is difficult because of the visual ambiguity between this decay and the decay  $\Sigma \rightarrow \Lambda e \nu$ , where the  $\Lambda$  decays via a neutral mode. The primary kinematic differences are due to the mass difference between the decay baryons; for the decay  $\Sigma \rightarrow \Lambda e \nu$  the electron momentum must be less than 80 MeV/c, whereas for  $\Sigma \rightarrow ne \nu$  the electron momentum can be as large as 240 MeV/c. Any positron coming from  $\Sigma^+$  decay with a momentum greater than 80 MeV/c would be clear evidence for  $\Sigma^+ \rightarrow ne^+ \nu$ ; none were seen. Two events were found with electron momenta of 18 and 24 MeV/c. Since six  $\Sigma^+ \rightarrow \Lambda e \nu$  events were found with visible  $\Lambda$  decays, we can expect three events with no visible  $\Lambda$ , and we thus conclude that we have not observed any examples of the decay  $\Sigma^+ \rightarrow ne^+ \nu$ .

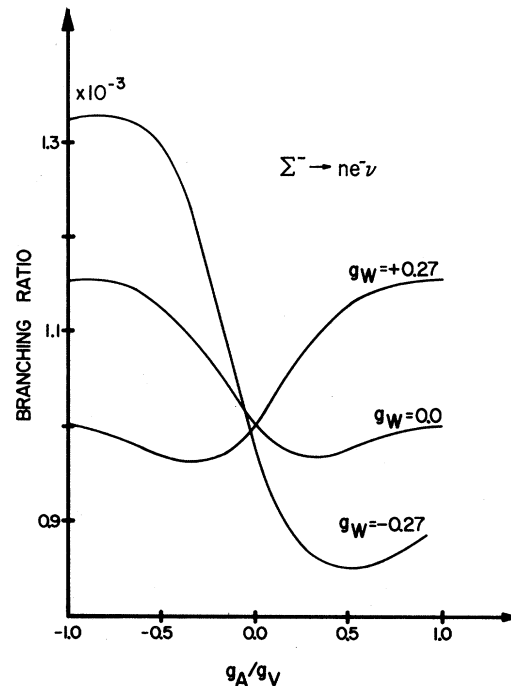


FIG. 3. Experimental branching ratio for  $\Sigma \rightarrow ne \nu$  as a function of  $g_A/g_V$  for selected values of the weak magnetism coupling constant.

The effectiveness of the  $\Delta S = \Delta Q$  selection rule is best indicated by a ratio of the decay rates of the two decays:

$$\frac{r(\Sigma^+ \rightarrow nev)}{r(\Sigma^- \rightarrow nev)} = \frac{R(\Sigma^+ \rightarrow nev)/\tau_{\Sigma^+}}{R(\Sigma^- \rightarrow nev)/\tau_{\Sigma^-}}$$

Less restrictive visibility criteria than for the  $\Sigma^- \rightarrow nev$  branching ratio yielded 133  $\Sigma^- \rightarrow ne^- \nu$  events. Then for equal scanning efficiencies, we have

$$\frac{r(\Sigma^+ \rightarrow nev)}{r(\Sigma^- \rightarrow nev)} = \frac{[(2-3)/0.96 \times 10^6] \times 1.49 \times 10^{-10}}{(133/2.12 \times 10^6) \times 0.81 \times 10^{-10}}$$

Using the statistical error on the two  $\Sigma^+$  electronic decays with no visible  $\Lambda^0$  and the six identifiable  $\Sigma^+ \rightarrow \Lambda e^+ \nu$  events, and adding the errors in quadrature, yields the result that the  $\Sigma^+ \rightarrow ne^+ \nu$  decay rate is less than 12% of the  $\Sigma^- \rightarrow nev$  decay rate with a confidence level of 95%.

#### VI. THE DECAY $\Sigma^- \rightarrow n\mu^- \nu$

The experimental observation of muon decays from  $\Sigma^-$  encounters several obstacles. In a scan the only reliable method of distinguishing muons from pions is the eventual decay of muons into electrons ( $\mu^\pm \rightarrow e^\pm \nu_e \nu_\mu$ ). Because of the relatively long  $\mu$  lifetime ( $2.2 \times 10^{-6}$  sec), this decay characteristically occurs after the muon has stopped. The electron from muon decay has a maximum momentum of 52.8 MeV/c, so most of the electrons are visible because of their spiral configuration or ionization. The scanners were instructed to look for all  $\Sigma^\pm$  decays which terminate in an obvious muon decay into an electron.

However, the common pionic  $\Sigma^\pm$  decays ( $\Sigma^\pm \rightarrow n\pi^\pm$ ) can give rise to muons through  $\pi \rightarrow \mu \nu$  decays. If the pion decays with the muon going either forward

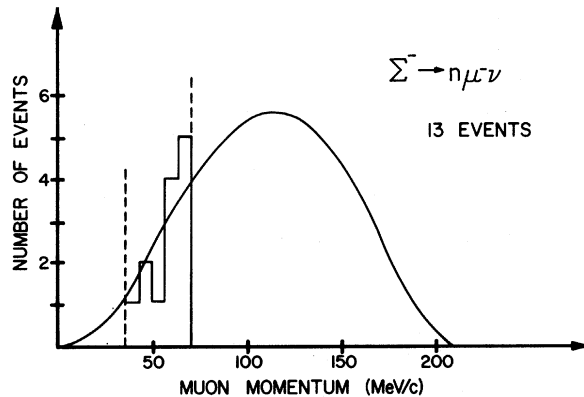


FIG. 4. Muon momentum spectrum for  $\Sigma^- \rightarrow n\mu^- \nu$  decays in the  $\Sigma^-$  center-of-mass frame. Only muons with a momentum between 35 and 70 MeV/c are used for computing the branching ratio.

or backward in the  $\pi$  center-of-mass system, the decay vertex is not visible and the pion is mistaken for a muon; these events must be removed. Two-body kinematics shows that all muons produced from nonradiative pion decays must have a momentum of at least 80 MeV/c. Since the muons coming from  $\Sigma^\pm \rightarrow n\mu^\pm \nu$  and from pionic decays cannot be separated, all muons with a lab momentum greater than 80 MeV/c must be discarded. Radiative pionic decays are largely removed by the same criterion. We estimate a remaining background of less than  $\frac{1}{10}$  of an event.

The measured length of the muon is used to determine the initial momentum which is compared to the momentum computed from the curvature of the track. The two measurements of the momentum are required to be within 2 standard deviations or the event is rejected. In order to compute a reliable curvature the muon must have at least 35 MeV/c initial momentum.

A Monte Carlo program was written to investigate the effects of these various selections. The same selections are made on the  $\Sigma^- \rightarrow n\mu^- \nu$  events as on the  $\Sigma^- \rightarrow nev$  events, with the addition of the requirement that the muon decay into an electron. Electrons from muon decay which failed to turn through at least  $180^\circ$  were rejected as were electrons of less than 12 MeV/c because of low scan-

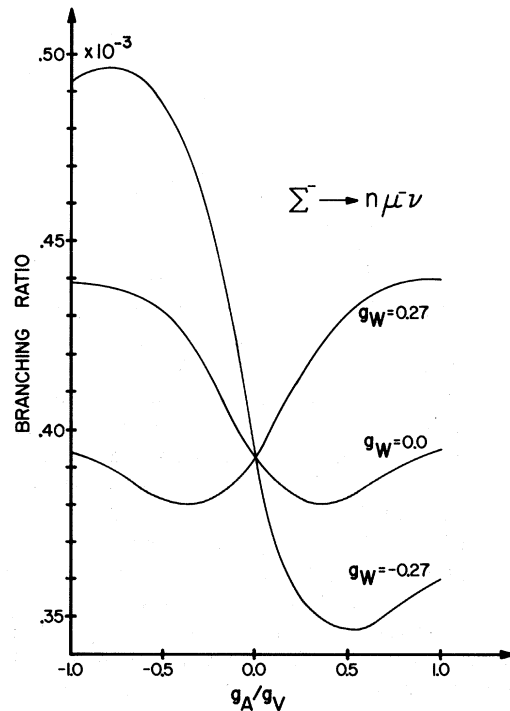


FIG. 5. Experimental branching ratio for  $\Sigma^- \rightarrow n\mu^- \nu$  as a function of  $g_A/g_V$  for selected values of the weak magnetism coupling constant.

ning efficiencies. After these restrictions 21.6% of the muon candidates remain. The expected fraction detected is calculated in a manner similar to that for  $\Sigma \rightarrow ne\nu$ , except that the muon events must have a muon momentum between 35 and 70 MeV/c in the  $\Sigma$  center-of-mass system. See Fig. 4.

There remain 13 events after the constraints; the scanning efficiency for these events is 70%. The branching ratio becomes

$$R(\Sigma^- \rightarrow n\mu\nu) = 13 \frac{1}{1.82 \times 10^6} \times \frac{1}{0.70} \times \frac{1}{0.216} \times \frac{1}{\text{fraction where } e^- \text{ turns more than } 180^\circ}$$

Figure 5 illustrates the dependence of the branch-

ing ratio on  $g_A/g_V$  for selected values of  $g_w$ . Using currently accepted values for the coupling constants,<sup>6</sup>  $g_A/g_V = -0.30$  and  $g_w = 0.27$ , the branching ratio becomes

$$R(\Sigma^- \rightarrow n\mu\nu) = (0.38 \pm 0.11) \times 10^{-3}.$$

These results are in good agreement with recent results at Maryland,<sup>7</sup> Princeton,<sup>8</sup> and Heidelberg.<sup>9</sup>

#### ACKNOWLEDGMENTS

We would like to thank the staffs of the Brookhaven AGS and the 30-in. bubble chambers for their help during the run, and Dr. David Berley, in particular, for the design and construction of the stopping  $K^-$  beam. We are truly grateful to the scanning staffs at Columbia and Stony Brook for their herculean efforts on this experiment.

\*Research supported by the U. S. Atomic Energy Commission.

†Present address: Bell Telephone Laboratory, Murray Hill, N. J.

‡Present address: State University of New York at Binghamton, Binghamton, N. Y.

<sup>1</sup>F. Eisler, R. Plano, A. Prodell, N. Samios, M. Schwartz, J. Steinberger, M. Conversi, I. Mannelli, R. Santangelo, and V. Silvestrini, Phys. Rev. **112**, 979 (1958).

<sup>2</sup>N. Cabibbo, Phys. Rev. Letters **10**, 531 (1963).

<sup>3</sup>J. Canter, J. Cole, J. Lee-Franzini, R. J. Loveless, C. Baltay, J. Feinman, P. Franzini, R. Newman, and

N. Yeh (unpublished).

<sup>4</sup>R. J. Loveless, thesis, SUNY at Stony Brook, 1969 (unpublished).

<sup>5</sup>W. E. Humphrey and R. R. Ross, Phys. Rev. **127**, 1305 (1962).

<sup>6</sup>F. Eisele, R. Engelman, H. Filthuth, W. Föhlisch, V. Hepp, E. Leitner, W. Presser, H. Schneider, and G. Zech, Z. Physik **225**, 383 (1969).

<sup>7</sup>N. V. Baggett *et al.*, Phys. Rev. Letters **23**, 249 (1969).

<sup>8</sup>E. Bierman *et al.*, Phys. Rev. Letters **20**, 1459 (1968).

<sup>9</sup>G. Ang *et al.*, Z. Physik **228**, 151 (1969).

## Calculated Cosmic-Ray Muon Spectra at High Energies (>20 GeV)

Keran O'Brien

Health and Safety Laboratory, U. S. Atomic Energy Commission, New York, New York 10014

(Received 16 December 1970; revised manuscript received 21 January 1971)

Calculations of sea-level cosmic-ray muon spectra have been made at 75°, 80°, 85°, and 88.75° between 20 and 1000 GeV, and compared with measurements made at Argonne National Laboratory. Although the experimental results are a consistent 60% of the calculated values, leading to too few muons being found at high zenith angles, it is felt that this does not support the Utah anomaly, as the discrepancy is energy- and angle-independent. Similarly, no exotic processes, such as the failure of special relativity, seem to be operating.

### I. INTRODUCTION

Cosmic rays are the only source of information on nucleon-nucleus collisions at energies above those available from accelerators. Pion partial

inelasticities, cross-section energy dependence, possible production processes, and the primary nucleon flux incident on the earth's atmosphere have, in the past, been estimated on an approximate basis from the dependence of muon fluxes